その分子メカニズムの解明が期待されている。

c）ZP4、PLXDC2、DKFZp762A217

日本人を対象とした全ゲノム相関解析による原発開放隅角緑内障の感受性遺伝子として、6つのSNPが染色体1（ZP4）、10（PLXDC2）、12（DKFZp762A217）において（p= 1 -9.0 x 10-5, OR=1.33-1.49）相関を示したと報告された[15]。しかしインドでの追試では再現性はとれていない。

3）緑内障と変更遺伝子

その他に単一遺伝子内のSNPを対象とした緑内障患者と健常者との相関解析（Case-control association study）では多数の遺伝子が報告されている（表2）。アルツハイマー病の発症に関係するアポリポタンパク質（Apolipoprotein E, ApoE）のプロモーター（転写制御領域）内のSNP（-219G）は視神経乳頭の障害と相関している。さらにApoEは変更遺伝子としてミオシリンに作用して緑内障を発症させると報告されている。変更遺伝子（Modifier gene）とは他の遺伝子の機能に影響力を持つ遺伝子である[16]。同様な関係がTNF-αとオプチニュリンの遺伝子多型でも報告されている[17]。

4）緑内障を再現するモデル動物と遺伝子改変モデル動物

緑内障研究においてモデル動物の存在はきわめて重要である。モデル動物を使って隅角や視神経網膜における変化を経時的に観察できること、さらに薬効評価に利用できることである。これまでにも自然発症や外科的手術によって複数のモデル動物が報告されている。動物種の選択は主にヒトとの視覚形態の類似性、発症までの時間、遺伝子操作の可能性、モデル動物の解析に必要な技術の整備、モデル動物の有効性、モデル動物の維持・管理に要する費用などによって選択されている。しかし、原因遺伝子や感受性遺伝子の解析となると遺伝子操作に適しているマウスが広く利用されている。

a）ラットモデル

動物モデルを用いて薬効評価を行う場合に多数の動物を用意する必要があるが、このような場合には一般的にラットが用いられる。ラットは適当な眼球サイズや飼育の容易さから利用されており、眼球構造も緑内障の研究には適している。ラットにおける眼圧上昇は強膜静脈への生理食塩水の注入、インドインクを使った線維柱帯の光凝固、線維柱帯の光凝固、強膜静脈の焼灼などの方法が用いられるが、研究者には高い技術力が求められる。これらの方法によって眼圧上昇を最大約2倍まで一過性に上昇させることができる。眼圧上昇は通常数週間持続され、さらに2回目の光凝固を行うと、3週間以上の高眼圧を持続することも可能である。この眼圧上昇によってヒトに類似する視神経線維の萎縮や視神経乳頭の変化が観察できる。ラットモデルの登場によって、眼圧上昇にともなう電気生理学的研究、神経保護薬の開発、そして網膜組織を使った遺伝子発現解析なども可能になった。眼圧が25－45mmHgに上昇するRCS（Royal College of Surgeons）ラットも発見されており、神経節細胞死や視神経乳頭陥凹などが観察されている。しかし残念ながらRCSラットにはチロシンキナーゼ遺伝子に変異があり、視細胞に変性が起こることから、緑内

障モデルとして利用する場合には注意が必要である。

b）マウスモデル

緑内障のマウスモデルはラットモデルの陰で開発が遅れていたが、遺伝子改変技術の進歩によって目的とするトランスジェニックマウス（外来遺伝子を体内で発現）、ノックアウトマウス（内在遺伝子を欠損）、ノックインマウス（内在遺伝子の置換）などが容易に作製されるようになり、眼球サイズが小さいという欠点がありながらも、モデル動物として広く利用されている。また、マウスは他の哺乳類に比べてゲノムやプロテオームのデータベースが整備されており、代謝系や行動パターンにいたるまで詳細な情報を手に入れることができる。しかしマウスにも緑内障モデルとしての欠点が存在する。マウスとヒトでは神経乳頭周辺の血管構造が異なることや、篩状板が存在しないなどの違いがあり、眼球サイズが小さいことから、その取り扱いが難しい。最も信頼性の高い眼圧測定法としては、角膜の厚さに影響されない侵襲的な方法がある。圧力計に接続したガラス管の針をマウスの前房に差し込み、眼圧を測定する方法である。この方法によって、異なるマウスの系について10－20mmHgの眼圧差が存在することが明らかになった。これに対して非侵襲式の利点は多数のマウスの眼圧を短い時間で測定できることであるが、角膜の厚さに影響を受ける。何れの方法についても安定した結果を得るにはやはり訓練が必要である。緑内障遺伝子としてはミオシリン、チトクロムP4501B1、オプチニュリン、WDR36の遺伝子改変マウスが作製され、緑内障の発症機序解明の研究に利用されている。遺伝子改変マウスの利点は発症原因が明らかにされていること、外科手術による作製法に比べて表現型が安定していること、繁殖が容易にできることである（遺伝子によって繁殖能力が低下するものもあるが）。すでに複数の緑内障マウスが作製されているが、その一つにミオシリンのTyr437His変異を発現するトランスジェニックマウスがある。このマウスは正常マウスに比べて昼は2mmHg、夜は4mmHgの眼圧上昇が認められ、生後1年目には網膜神経節細胞数の20%が減少する[18]。コラーゲンタイプ1α1サブユニットに遺伝子変異のあるトランスジェニックマウスではコラーゲンのメタロプロテアーゼ（MMP1）による分解が阻害され、生後36週ほどかけて眼圧が4.8mmHg上昇することが報告されている。隅角の構造は保持されたまま、網膜神経節細胞層の障害が観察され、開放隅角緑内障マウスモデルとして認識されている。また、我々が作製したオプチニュリンGlu50Lys（E50K）変異体を発現したマウスでは、正常眼圧は維持されたまま、生後1年後には網膜神経節細胞死や視神経乳頭の陥凹が観察されている[10]。マウスの外科的手術による眼圧上昇はラットより技術的に困難である。C57BL/6Jマウスの前房にインドシアニングリーンを注入し、線維柱帯と上強膜静脈部位の光凝固を施すと約10日後に眼圧が正常なマウスの15.2 ± 0.6mmHgに対して33.6 ± 1.5mmHgに上昇するが、60日後には正常値に戻ると報告されている。網膜神経節細胞層や網膜への機能障害が網膜電図（ERG）などによって明らかにされている。Johnらによって報告されたDBA/2Jマウスは2つの遺伝子Tyrp1とGpnmb[11]に変異があり、色素顆粒の分散による虹彩の萎縮が起こり、虹彩癒着によって生後9ヶ月後には眼圧が上昇し、

視神経乳頭を基点として網膜神経節細胞死が扇状に観察されることがわかっている[12]。

c） 霊長類モデル

全ての動物モデルの中で隅角や視神経乳頭の構造がヒトと最も類似する霊長類モデルが研究に適していることは言うまでもないことである。特に房水流出機構に関する研究においては貴重な存在である。しかし、倫理的な正当性や一頭当たりの維持費用がマウスよりかかること、さらに飼育・管理に高度な知識・技術が必要であることから、多くの研究では利用されていない。房水流路の遮断には主に線維柱帯の光凝固が利用される[13]。この手法によって手術後数日間で25－60mmHgの眼圧上昇が期待できる。その他の手法としては前房内に赤血球、ラテックス粒子、ポリアクリルアミドゲル、酵素、ステロイド[22]を注入することによって眼圧上昇を促す研究例が報告されているが、光凝固によって最も安定した眼圧上昇が得られている[23]。霊長類における眼圧上昇は視神経乳頭、網膜神経線維、網膜神経節細胞層に障害[24]をもたらし、ヒトと同様な病理学的所見が再現されることが確認されている。また、霊長類モデルを利用した、光凝固後30日における網膜内の遺伝子発現の研究も報告されており[25]、この情報は新しい治療薬の開発にも応用されている。

d） ゼブラフィッシュ

眼における遺伝子の機能をすばやく調べる方法として、ゼブラフィッシュ（Zebrafish）を利用した研究が最近報告されており、ミオシリン、オプチニュリン、WDR36などの欠損による眼球への影響が報告されている（図4）。

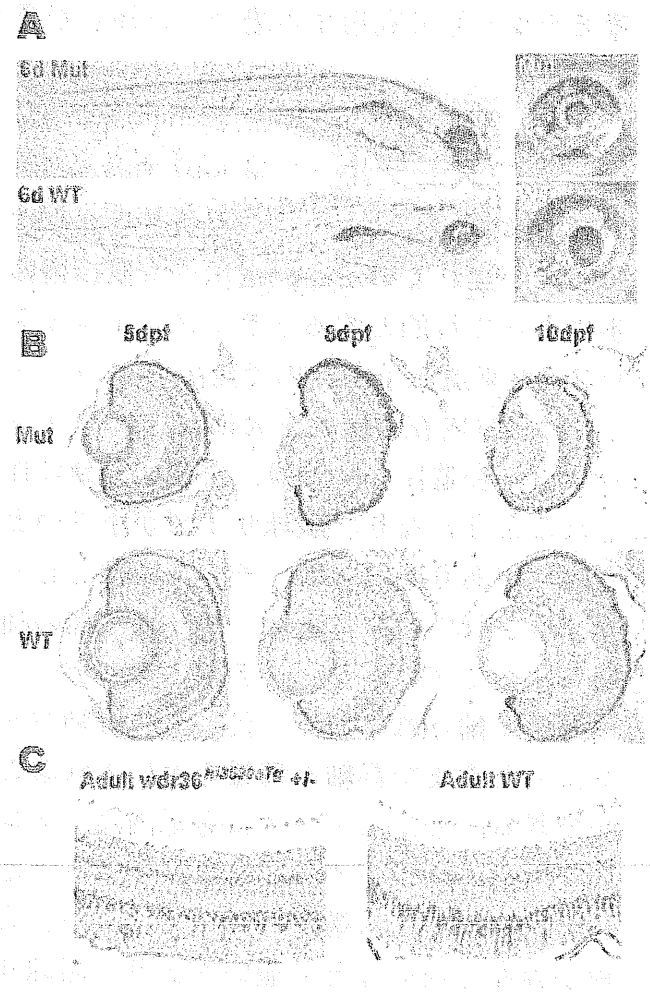

図4　WDR36を欠損したゼブラフィッシュにおける眼球の異常
WDR36欠損ゼブラフィッシュ（Mut）は正常ゼブラフィッシュ（Wt）に比べて眼球の形成に異常がある[12]

終わりに

ミオシリンの発見から緑内障の遺伝子研究は大きく前進し、複数の原因遺伝子や感受性遺伝子が発見されている。しかしそれぞれ単独の遺伝子だけでは緑内障の発症を説明することはできない。近年このような多因子疾患を説明する理論としてCommon disease rare variant説がある。これは発症頻度の高い疾患が実は稀に表れる複数個の遺伝子変異（ある

いは遺伝子多型）の組み合わせで発症するという説である。これらの稀に表れる遺伝子（変異）多型を抽出するには全ゲノム相関解析の規模を数万人単位に増やすか、日本人を対象とした家族性の緑内障遺伝子を積極的に探索する必要がある。現在我々は複数の緑内障家系を対象に研究を進めている。また、DNA配列を高速で解読する次世代型のDNAシークエンサー（塩基配列読み取り装置）の登場により、1人のゲノム配列を1日で1台のシークエンサーで読み取ることが可能になってきた。このスピードは今後さらに高速化されるであろう。読み取り価格も10万円である。遺伝子解析がゲノムレベルで解析され、論じられる時代に突入しており、緑内障研究もこのような大きな波の中で大きく前進すると期待される。

文　献

1）Stoilov I, Akarsu AN, Sarfarazi M. Identification of three different truncating mutations in cytochrome P4501B1 (CYP1B1) as the principal cause of primary congenital glaucoma (Buphthalmos) in families linked to the GLC3A locus on chromosome 2p21. Hum Mol Genet. 1997;6:641-7.

2）Vincent AL, Billingsley G, Buys Y, Levin AV, Priston M, Trope G, et al. Digenic inheritance of early-onset glaucoma: CYP1B1, a potential modifier gene. Am J Hum Genet. 2002;70:448-60.

3）Sheffield VC, Stone EM, Alward WL, Drack AV, Johnson AT, Streb LM, et al. Genetic linkage of familial open angle glaucoma to chromosome 1q21-q31. Nat Genet. 1993;4:47-50.

4）Fingert JH, Heon E, Liebmann JM, Yamamoto T, Craig JE, Rait J, et al. Analysis of myocilin mutations in 1703 glaucoma patients from five different populations. Hum Mol Genet. 1999;8:899-905.

5）Resch ZT, Fautsch MP. Glaucoma-associated myocilin: A better understanding but much more to learn. Exp Eye Res. 2009;88:704-12.

6）Fautsch MP, Vrabel AM, Johnson DH. The identification of myocilin-associated proteins in the human trabecular meshwork. Exp Eye Res. 2006;82:1046-52.

7）Jacobson N, Andreswsm M, Shepard AR, Nishimura D, Searby C, Fingert JH, et al. Non-secretion of mutant proteins of the glaucoma gene Myocilin in cultured trabecular meshwork cells and in aqueous humor. Hum Mol Genet. 2001;10:117-25.

8）Sarfarazi M, Child A, Stoilova D, Brice G, Desai T, Trifan OC, et al. Localization of the fourth locus (GLC1E) for adult-onset primary open-angle glaucoma to the 10p15-p14 region. Am J Hum Genet. 1998;62:641-52.

9）Rezaie T, Child A, Hitchings R, Brice G, Miller L, Coca-Prados M, et al. Adult-onset primary open-angle glaucoma caused by mutations in optineurin. Science. 2002;295:1077-9.

10）Chi Z-L, Akahori, A, Obazawa M, Minami M, Noda T, Nakaya N, Tomarev S, Kawase K, Yamamoto T, Noda S, Sasaoka M, Shimazaki A, Takada Y, and Iwata T. Overexpression of optineurin E50K disrupts

Rab 8 interaction and leads to a progressive retinal degeneration in mice. Human Molecular Genetics. 2010; 19:2605-15.
11) Monemi S, Spaeth G, DaSilva A, Popinchalk S, Ilitchev E, Liebmann J, et al. Identification of a novel adult-onset primary open-angle glaucoma (POAG) gene on 5 q22.1. Hum Mol Genet. 2005;14:725-33.
12) Skarie JM, Link BA. The primary open-angle glaucoma gene WDR36 functions in ribosomal RNA processing and interacts with the p53 stress-response pathway. Hum Mol Genet. 2008;17:2474-85.
13) Thorleifsson G, Magnuson KP, Sulem P, Walters GB, Gudbjartsson DF, Stefansson H, et al. Common sequence variants in the LOXL 1 gene confer susceptibility to exfoliation glaucoma. Science. 2007;317:1397-400.
14) Thorleifsson G, Walters GB, Hewitt AW, Masson G, Helgason A, DeWan A, Sigurdsson A, Jonasdottir A, Gudjonsson SA, Magnusson KP, Stefansson H, Lam DS, Tam PO, Gudmundsdottir GJ, Southgate L, Burdon KP, Gottfredsdottir MS, Aldred MA, Mitchell P, St Clair D, Collier DA, Tang N, Sveinsson O, Macgregor S, Martin NG, Cree AJ, Gibson J, Macleod A, Jacob A, Ennis S, Young TL, Chan JC, Karwatowski WS, Hammond CJ, Thordarson K, Zhang M, Wadelius C, Lotery AJ, Trembath RC, Pang CP, Hoh J, Craig JE, Kong A, Mackey DA, Jonasson F, Thorsteinsdottir U, Stefansson K. Common variants near CAV 1 and CAV 2 are associated with primary open-angle glaucoma. Nat Genet. 2010;42:906-9.
15) Nakano M, Ikeda Y, Taniguchi T, Yagi T, Fuwa M, Omi N, et al. Three susceptible loci associated with primary open-angle glaucoma identified by genome-wide association study in a Japanese population. Proc Natl Acad Sci USA. 2009;106:12838-42.
16) Copin B, Brézin AP, Valtot F, Dascotte JC, Béchetoille A, Garchon HJ. Apolipoprotein E promoter singlenucleotide polymorphisms affect the phenotype of primary open angle glaucoma and demonstrate interaction with the myocilin gene. Am J Hum Genet. 2002;70:1575-81.
17) Funayama T, Ishikawa K, Ohtake Y, Tanino T, Kurosaka D, Kimura I, et al. Variants in optineurin gene and their association with tumor necrosis factor-alpha polymorphisms in Japanese patients with glaucoma. Invest Ophthalmol Vis Sci. 2004;45:4359-67.
18) Senatorov VV, Malyukova I, Fariss R, Wawrousek E, Swaminathan S, Sharan SK, Tomarev S. Expression of mutated mouse myocilin induces open-angle glaucoma in transgenic mice. J. Neurosci. 2006;26:11903-14.
19) Anderson MG, Smith RS, Hawes NL, Zabaleta A, Chang B, Wiggs JL et al. Mutations in genes encoding melanosomal proteins cause pigmentary glaucoma in DBA/ 2 J mice. Nat Genet 2002;30:81-85.
20) Jakobs TC, Libby RT, Ben Y, John SW, Masland RH. Retinal ganglion cell degeneration is topological but not cell type specific in DBA/ 2 J mice. J Cell Biol 2005;171:313-325.

21) Gaasterland D, Kupfer C. Experimental glaucoma in the rhesus monkey. Invest Ophthalmol Vis Sci 1974;13:455-457.
22) Amfrmaly MF. Aqueous outflow facility in monkeys and the effect of topical corticoids. Invest Ophthalmol 1964; 3 :534-538.
23) Rasmussen CA, Kaufman PL. Primate glaucoma models. J Glaucoma 2005;14:311-314.
24) Quigley HA, Nickells RW, Kerrigan LA, Pease ME, Thibault DJ, Zack DJ. Retinal ganglion cell death in experimental glaucoma and after axotomy occurs by apoptosis. Invest Ophthalmol Vis Sci 1995;36:774-786.
25) Miyahara T, Kikuchi T, Akimoto M, Kurokawa T, Shibuki H, Yoshimura N. Gene microarray analysis of experimental glaucomatous retina from cynomologous monkey. Invest Ophthalmol Vis Sci 2003;44:4347-4356.

HMG Advance Access published May 21, 2013

Human Molecular Genetics, 2013 **1–9**
doi.10.1093/hmg/ddt210

Enhanced optineurin E50K–TBK1 interaction evokes protein insolubility and initiates familial primary open-angle glaucoma

Yuriko Minegishi[1], Daisuke Iejima[1], Hiroaki Kobayashi[1], Zai-Long Chi[1], Kazuhide Kawase[2], Tetsuya Yamamoto[2], Tomohisa Seki[3], Shinsuke Yuasa[3], Keiichi Fukuda[3] and Takeshi Iwata[1,*]

[1]Division of Molecular and Cellular Biology, National Institute of Sensory Organs, National Hospital Organization Tokyo Medical Center, Tokyo, Japan [2]Department of Ophthalmology, Gifu University School of Medicine, Gifu, Japan [3]Department of Cardiology, Keio University School of Medicine, Tokyo, Japan

Received March 13, 2013; Revised April 15, 2013; Accepted May 1, 2013

Glaucoma is the leading cause for blindness affecting 60 million people worldwide. The optineurin (OPTN) E50K mutation was first identified in familial primary open-angle glaucoma (POAG), the onset of which is not associated with intraocular pressure (IOP) elevation, and is classified as normal-tension glaucoma (NTG). Optineurin (OPTN) is a multifunctional protein and its mutations are associated with neurodegenerative diseases such as POAG and amyotrophic lateral sclerosis (ALS). We have previously described an E50K mutation-carrying transgenic (E50K^{-tg}) mouse that exhibited glaucomatous phenotypes of decreased retinal ganglion cells (RGCs) and surrounding cell death at normal IOP. Further phenotypic analysis of these mice revealed persistent reactive gliosis and E50K mutant protein deposits in the outer plexiform layer (OPL). Over-expression of E50K in HEK293 cells indicated accumulation of insoluble OPTN in the endoplasmic reticulum (ER). This phenomenon was consistent with the results seen in neurons derived from induced pluripotent stem cells (iPSCs) from E50K mutation-carrying NTG patients. The E50K mutant strongly interacted with TANK-binding kinase 1 (TBK1), which prohibited the proper oligomerization and solubility of OPTN, both of which are important for OPTN intracellular transition. Treatment with a TBK1 inhibitor, BX795, abrogated the aberrant insolubility of the E50K mutant. Here, we delineated the intracellular dynamics of the endogenous E50K mutant protein for the first time and demonstrated how this mutation causes OPTN insolubility, in association with TBK1, to evoke POAG.

INTRODUCTION

Glaucoma is one of the world's leading cause of adult-onset blindness that causes optic nerve degeneration characterized by progressive and irreversible loss of retinal ganglion cells (RGCs) and retinal nerve fiber layer defects accompanied by the corresponding visual field damage (1). Open-angle glaucoma, the most prevalent subtype among various glaucomas, is further subdivided into two major types according to intraocular pressure (IOP). In the high-IOP type or primary open-angle glaucoma (POAG), elevated IOP due to disturbance of aqueous humor outflow in the trabecular meshwork or Schlemm's canal mechanically damages RGCs (2). In the normal-IOP type or normal-tension glaucoma (NTG), IOP elevation does not necessarily cause glaucoma, but some IOP-independent factors are thought to be involved (2). According to a population-based glaucoma survey conducted in Japan, NTG is the most prevalent subtype of glaucoma in the country (3, 4). This epidemiological study in Japan reported that the subjects' average IOP was ~15 mmHg and the POAG prevalence was almost equivalent in groups with IOP higher or lower than the average IOP (4). We have investigated the onset mechanism of the latter glaucoma subset, with lower IOP than average, as NTG. Interestingly enough, IOP-unrelated genetic mutations have been found recently in NTG (5, 6) and the Optineurin (OPTN) E50K mutation was the first one identified in familial NTG (7).

OPTN, a scaffold protein with various biological functions, has a few coiled-coil domains and a ubiquitin-binding domain

*To whom correspondence should be addressed at. Division of Molecular and Cellular Biology, National Institute of Sensory Organs, National Hospital Organization Tokyo Medical Center, 2-5-1 Higashigaoka, Meguro-ku, Tokyo 152-8902, Japan. Tel/Fax. +81 334111026; Email iwatatakeshi@kankakuki.go.jp

at C-terminal. It associates with membrane trafficking proteins Myosin VI and Rab 8 to form Golgi ribbons and is involved in exocytosis (8, 9). And thus E50K mutation yields several phenotypes, such as fragmentation of Golgi apparatus (10), transport failure (8, 11) or apoptotic cell death (12, 13).

OPTN also participates in innate immunity response by regulating NF-κB activation and autophagy in anti-infection processes (14, 15) and via its interaction with some other proteins (16). Among the several OPTN mutations described in the original report, the role of a glutamic acid-to-lysine conversion at amino acid 50 (E50K) in NTG is well accepted worldwide (17–19). A family with a history of NTG was previously identified with the E50K mutation, and in affected members of this family, visual failure starts at about the age of 30 years (Supplementary Material, Fig, S1) and progresses to glaucoma without elevation of IOP until vision is entirely lost at about the age of 70 years (19) Recently, Maruyama *et al.* (20) identified three additional mutations in *OPTN*, a deletion in exon 5, a nonsense mutation (Q398X) and a missense mutation (E478G) that was associated with amyotrophic lateral sclerosis (ALS). Among these three mutations, the former two were recessive mutations and the latter E478G mutation was a dominant mutation, like E50K. The authors further showed the attenuation of the inhibitory effect of NF-κB activation by OPTN carrying the E478G mutation, but that the inhibitory function remained intact with the E50K mutation. Though the underlying causes of OPTN mutation-driven changes are different in POAG and ALS, it is still intriguing that OPTN plays crucial roles in neural homeostasis.

All these results suggest that the E50K mutant expression restricts retinal neural cell survival and is thus involved in the progression of POAG. The underlying molecular mechanism of how the glaucoma phenotype is evoked by a single amino acid replacement in OPTN is still unknown.

In this study, we further characterized the effects of the E50K mutation in OPTN in E50K transgenic ($E50K^{tg}$) mice and explored the endogenous OPTN dynamics in neural cells differentiated from induced pluripotent stem cells (iPSCs) derived from NTG patients with the genetic mutation corresponding to E50K. At the molecular level, abnormal insolubility of the endogenous E50K OPTN mutant was demonstrated in this study for the first time. This insolubility was simultaneously attributed to the formation of a distinct protein complex, and to disabled oligomerization of OPTN, associated with an enhanced E50K–tank-binding kinase (TBK)1 interaction. The abnormal insolubility of the E50K mutant was rescued by treatment with a TBK1-specific inhibitor.

RESULTS

OPTN E50K transgenic mice exhibit profound gliosis in the retina

In our previous report, we showed that $E50K^{tg}$ mice exhibited phenotypes, such as a decreased number of RGCs and progressive diminution of retinal thickness without elevation of IOP (19). Immunohistochemistry of the flat-mount retinas of $E50K^{tg}$ mice showed persistent glial fibrillary acidic protein (GFAP)-positive dot-staining between astrocytes, compared with the staining pattern in retinas of wild-type mice (Fig 1A and B). Evaluation of the pathological condition in age-matched wild-type and mutant mice by pathologists blinded to the sample source indicated significantly increased gliosis in the $E50K^{tg}$ mice, compared with the wild-type mice (Fig 1C). GFAP-positive Müller cells are known as one of the hallmarks for retinal neurodegenerative conditions, including glaucoma (21), which can be simulated by various retinal insults such as the optic nerve axonal damage, laser ablation and intravitreal injection of kainic acid (22–24). From the morphological analysis of the cells that appeared in the vertically incised retinal surface (Fig. 1D, dashed line), the GFAP-positive dots shown in the flat-mount specimen were concluded to be Müller cells, from their peculiar spindle shape (Fig. 1D, arrowheads) Reactive gliosis has been reported to be associated with retinal physical insults; thus, this phenotype in $E50K^{tg}$ mice in the absence of physical insults was of particular interest. Therefore, in addition to the reactive gliosis in the retinas of $E50K^{tg}$ mice, the retinal vessels were examined by *z*-axis confocal laser microscopy after tail vein injection of red fluorescent dye-conjugated isolectin. The confocal microscopy images revealed a number of gliosis scars embracing leakage of isolectin from vessels (Supplementary Material, Fig. S2A). These findings suggest that the retinas of $E50K^{tg}$ mice are under continuous stress and are structurally vulnerable.

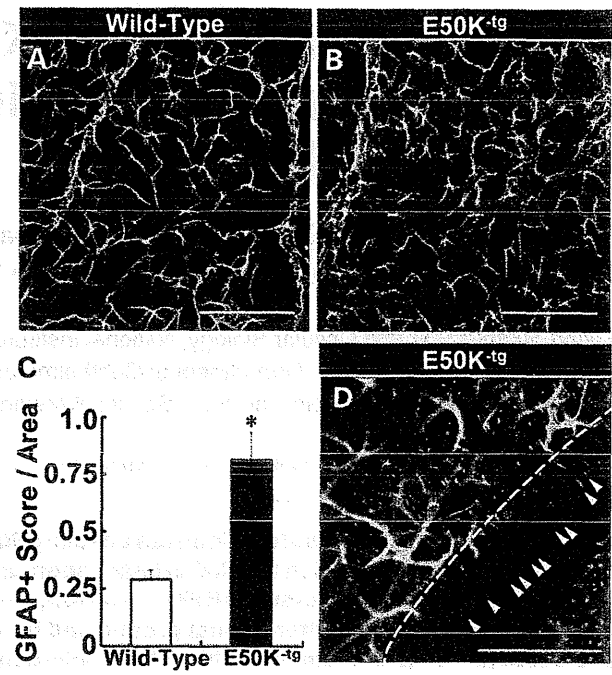

Figure 1. Persistent reactive gliosis in E50K-transgenic ($E50K^{tg}$) mouse retinas. Representative retinal flat-mount immunohistochemistry images of anti-GFAP in (**A**) wild-type and (**B**) $E50K^{tg}$ mice. Scale bar = 200 μm. Flat-mount specimens were analyzed (blinded evaluation) for gliosis assessment. The scores of GFAP-positive gliosis area/retinal area are plotted (data are mean ± SD; four fields of micrographs were chosen randomly and analyzed from one specimen, $n = 4$, $^*P < 0.05$). (**D**) The appearance of GFAP-positive Müller cells in $E50K^{tg}$ mice. The dashed line indicates the border of the retinal luminal surface and the incised surface of the retina; arrowheads indicate the feet of GFAP-positive astrocytes. Scale bar = 100 μm. Some of the gliosis harbors the retinal vessel leakage (Supplementary Material, Fig. S1A).

OPTN E50K protein accumulates in the outer plexiform layer of the retinas of E50K^{-tg} mice

Considering the previous report of the deposit-like pathology in motor neurons in the ALS-associated OPTN E478G mutation (20), we also investigated the localization of the OPTN E50K protein in the retinas of E50K^{-tg} mice by immunohistochemistry. Negative control slides, treated with rabbit IgG cocktail alone, did not exhibit significant signals (Fig. 2A and B), while the retinas of E50K^{-tg} mice exhibited positive staining for OPTN in the outer plexiform layer (OPL) and the inner nuclear layer (INL), as small dot-like deposits (Fig. 2D and F, arrows). The retinas of wild-type littermates did not exhibit such a pattern (Fig. 2C and E). We designed this transgenic mouse with N-terminally HA-tagged OPTN protein, which would enable us to confirm whether the deposits include E50K mutant protein. HA-tagged E50K was mainly detected in the OPL of the retinas in E50K^{-tg} mice, which was consistent with the immunostaining results with the anti-OPTN antibody (Supplementary Material, Fig. S3D, arrows). Positive signals were not detected for OPTN in control slides in the retinas of wild-type mice and in those treated with the IgG alone (Supplementary Material, Fig. S3A–C). Thus, OPTN deposits in the retinas of E50K^{-tg} mice were caused exclusively from the expression of the E50K mutant. These pathology findings point to the capacity of the E50K mutant protein to aggregate.

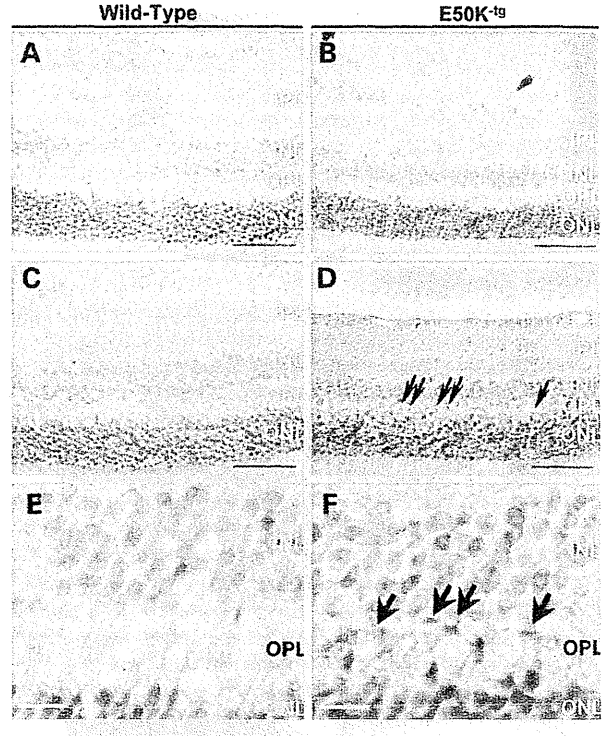

Figure 2. E50K mutant protein deposits in the retinas of E50K^{-tg} mice. (**A**) Rabbit IgG negative control for the immunohistochemistry analysis of the retina of a wild-type mouse. (**B**) Rabbit IgG negative control for the immunohistochemistry analysis of the retina of an E50K^{-tg} mouse. Both negative control slides showed minimum background staining. (**C**) Anti-OPTN immunohistochemistry of the wild-type mouse retina. Moderate OPTN signals were detected in luminal to inner layers of the retina. (**D**) Anti-OPTN immunohistochemistry of the E50K^{-tg} mouse. In addition to the moderate OPTN signals similar to that in the wild-type mouse retina, some strong deposit-like signals from INL to OPL were detected (indicated with arrows). Scale bars = 50 μm. High magnification micrograph of the retina of (**E**) wild-type and (**F**) E50K^{-tg} mice. Arrows indicate the OPTN deposit-like signals. Scale bars = 10 μm. The OPTN signals consists of, at least to some extent, the E50K^{-tg} transgene product, from the results of immunohistochemistry analysis with an anti-HA antibody (Supplementary Material, Fig. S2D). INL, inner nuclear layer; OPL, outer plexiform layer; ONL, outer nuclear layer.

Examination of induced neural cells from NTG patient-derived iPSCs indicates disturbed OPTN transition from ER to Golgi and Golgi body constriction

To clarify the cause of E50K mutant protein deposits in the retinas of E50K^{-tg} mice, we first examined the intracellular localization of wild-type OPTN and the E50K mutant by transfecting vectors encoding the two proteins fused with enhanced green fluorescent protein (EGFP) (^{EGFP}-OPTN and ^{EGFP}-E50K, respectively) into HEK 293 cells. ^{EGFP}-OPTN could be seen as small puncta widely distributed intracellularly, while ^{EGFP}-E50K was seen as larger puncta accumulated in the perinuclear region, and the Golgi body in the E50K-expressing cells was fragmented (Supplementary Material, Fig. S4B, arrowheads) as previously reported (10, 20). Since Golgi body formation and its membrane trafficking are associated with the endoplasmic reticulum (ER) (25, 26), ER structure was also examined using an ER detection kit (ER-ID, Enzo). Again, the wild-type OPTN was observed as small puncta dispersed within the cytosol (Fig. 3A), while the larger vesicles of the E50K mutant were accumulated in the perinuclear region surrounded by the ER membrane (Fig. 3B, arrows). To elucidate the intracellular localization of endogenous OPTN, we generated induced pluripotent stem cells (iPSCs) from peripheral blood mononuclear cells isolated from NTG patients with the mutation corresponding to E50K and examined OPTN localization in these cells. The pluripotency of iPSCs was confirmed by immunostaining with antibodies specific for Oct3 and Nanog, pluripotency markers (Supplementary Material, Fig. S5A). Neural induction was conducted as previously reported (27, 28) and neuronal differentiation was confirmed by staining with an antibody specific for Tuj1, a neuronal marker (Supplementary Material, Fig. S5B). iPSC-derived neural cells from NTG patients with the mutation corresponding to E50K were immunostained for OPTN and GM130, as a Golgi body marker, along with ER staining. In the iPSCs with wild-type OPTN, derived from a non-glaucoma subject, OPTN-associated vesicles were dispersed within the cells from ER to Golgi networks, in a pattern identical to that in HEK293 cells over-expressing wild-type OPTN (Fig. 3C). However, in the iPSCs from the NTG patient with the mutation corresponding to E50K, the number of OPTN-associated vesicles was decreased, compared with that in the control iPSCs, with dense aggregation in perinuclear regions and shrinkage of the ER/Golgi body (Fig. 3D). Upon microscopic examination under higher magnification, we found that wild-type OPTN frequently localized on the tips of Golgi ribbons (Fig. 3E), while the E50K OPTN mutant in iPSCs from NTG patients accumulated in the ER and Golgi body (Fig 3F). Co-localization of wild-type OPTN and the Golgi body was

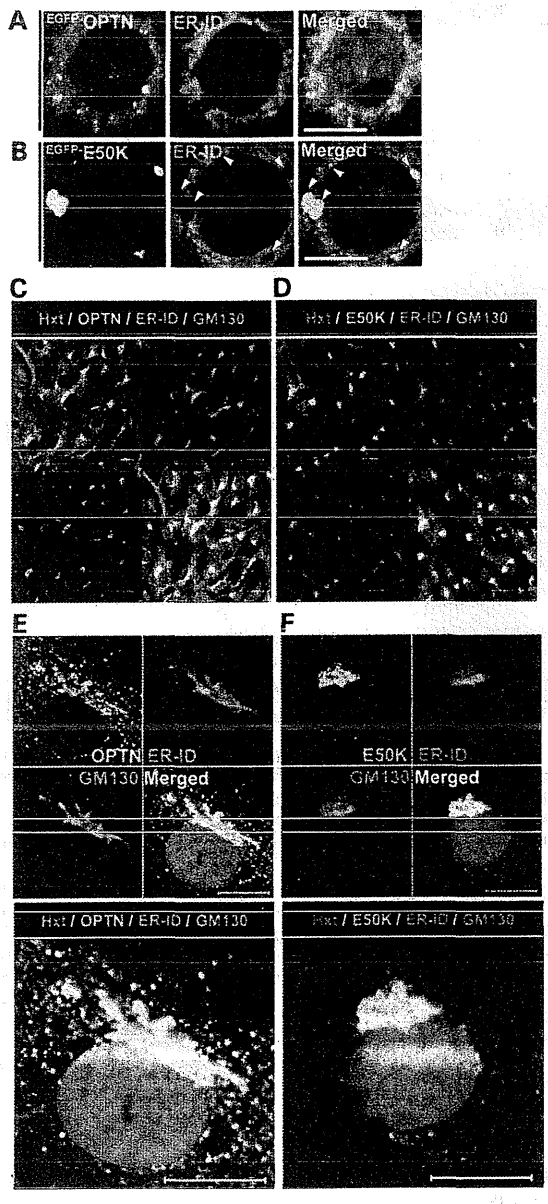

Figure 3. Distinct intracellular localization of wild-type OPTN and the E50K mutant. Intracellular localization of OPTN and E50K in over-expression studies. (**A**) ^{EGFP}-OPTN (green) and ER (red) localization 1 day after transfection. (**B**) ^{EGFP}-E50K mutant (green) and ER (red) localization 1 day after transfection. Both micrographs are shown with nuclear counter-staining with Hoechst 33342 (blue). Arrowheads indicate the E50K accumulation in the ER. Scale bars = 10 μm. iPSCs were established from iPSCs without the E50K mutation, derived from non-glaucoma subjects, as a control and with the E50K mutation, derived from glaucoma patients for endogenous analyses. Ten days after neural induction, OPTN (green), ER (red) and Golgi (magenta) co-localization were analyzed by immunocytochemistry. (**C**) Endogenous OPTN localization in neural control cells or (**D**) E50K glaucoma patient-derived neural cells. OPTN signals exhibited an accumulated pattern in cells with the E50K mutation. Higher magnification of endogenous OPTN signals in (**E**) control cells and (**F**) cells with the E50K mutation. In control cells, OPTN signals (green vesicles) were localized on the tips of ribbon Golgi body, while in the cells with the E50K mutation, the number of OPTN signals was decreased and largely accumulated within the ER and to a shrunken Golgi body (shown by the white signal in merged micrographs, respectively). All scale bars = 10 μm.

frequently observed (Supplementary Material, Fig. S4A, arrow), but such a co-localization was scarce for the E50K mutant (Supplementary Material, Fig. S4B). These results indicate that the expression of the E50K mutant affects OPTN transition from ER to Golgi body prior to Golgi shrinkage/fragmentation.

Insolubility of OPTN in iPSCs and iPSC-derived neural cells from NTG patients with the mutation corresponding to E50K

While performing the over-expression experiments, we noticed that the protein amount of over-expressed E50K was decreased to half that of wild-type OPTN in HEK293T cells. A similar result has been previously reported in dermal fibroblasts from the E50K mutation-carrying patients (29). Since there was no significant difference in the mRNA levels in both groups (Supplementary Material, Fig. S6A), we speculated that E50K is more susceptible to intracellular degradation. Our previous studies have shown that OPTN is degraded by proteasomal and lysosomal pathways (30). Therefore, we first treated cells with MG132, a proteasomal inhibitor, and bafilomycin, a lysosomal inhibitor, along with cycloheximide, a protein synthesis inhibitor, to compare the amount of protein degradation. The levels of over-expressed OPTN in cells treated only with cycloheximide were lower, while co-treatment with MG132 or bafilomycin restored the OPTN protein levels, as previously reported (Supplementary Material, Fig. S7A, OPTN lanes). However, over-expressed E50K mutant protein was not restored, unlike over-expressed wild-type OPTN, upon treatment of cells with inhibitors (Supplementary Material, Fig. S7A, E50K lanes) These results indicate that there was no association between the lower levels of the E50K mutant and intracellular degradation of OPTN. We predicted that E50K might be expressed at levels comparable to the wild-type protein, but was probably insoluble and was being precipitated with the insoluble pellet (Ppt.) fraction of the cell lysate after routine cell-lysate collection Although an equivalent amount of calnexin, a Ppt. marker, was detected in the Ppt. fraction of both wild-type- and E50K-expressing HEK293 cells, ~2- to 5-fold higher amounts of E50K protein, compared with the wild-type OPTN, was detected in the Ppt. fraction (Fig. 4A and B). The insolubilized E50K increased in an E50K expression-dependent manner (Fig. 4C). To elucidate the reason for this altered solubility of E50K mutant protein, we utilized the aforementioned iPSCs and examined the OPTN protein levels by western blotting. Although the OPTN expression was moderate in undifferentiated iPSCs, OPTN was detected in the Sup. fraction of control iPSC lysates (Fig. 4D, control 1–4), while OPTN was detected in the Ppt. fraction of iPSCs from NTG patients with the mutation corresponding to E50K (Fig. 4D, E50K 1–6). OPTN expression was significantly increased after neural induction (Fig. 4E Sup. lanes). The iPSC-derived neural cells recapitulated these results, i.e. abundant OPTN in the Ppt. fraction in E50K mutation-carrying NTG patient-derived cells (Fig. 4E, Ppt. lanes). These findings indicate that regardless of the expression levels, the E50K mutant protein exhibits higher intracellular insolubility.

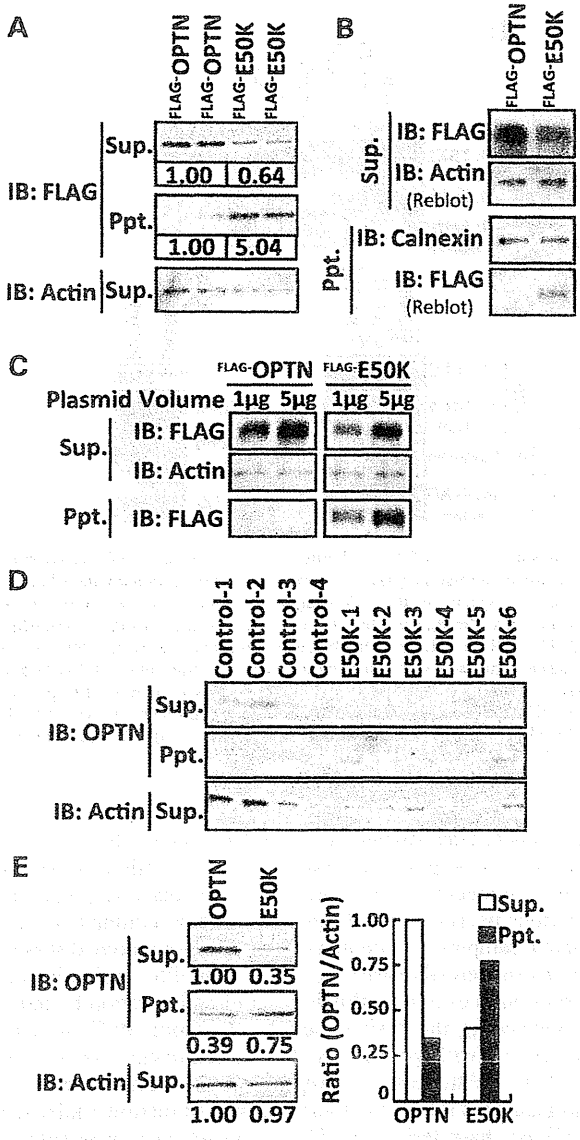

Figure 4. Distinct protein solubility of wild-type OPTN and the E50K mutant. (**A**) Wild-type OPTN and E50K expression under the same transfection condition. There were no differences in mRNA expressions under these transfection conditions (Supplementary Material, Fig. S4A). The 'Missing' E50K mutant protein was detected in the precipitated fraction (Ppt.), after supernatant (Sup.) collection. Semi-quantitative western blotting analysis was performed using Chemidoc (BioRad) with imaging software and the results are shown under each band. Approximately 2-fold reduction of E50K mutant protein in the Sup. fraction and 2- to 5-fold induction in the Ppt. fraction were observed. (**B**) Although calnexin, an ER membrane marker, is detected in both the Ppt. fraction of wild-type OPTN-expressing and E50K mutant-expressing cells, only the E50K mutant is detected in the Ppt. fraction. (**C**) The E50K mutant in the Ppt. fraction was increased in an E50K expression-dependent manner (**D**) Endogenous expression and higher hydrophobicity of OPTN in iPSCs with the E50K mutation. Endogenous OPTN is also detected in the Ppt. fraction in iPSCs from E50K mutation-carrying NTG patients. (**E**) Abundant endogenous expression and higher hydrophobicity of OPTN in iPSC-derived neural cells 10 days after induction from E50K mutation-carrying NTG patients. Semi-quantitative western blotting analysis by Chemidoc with imaging software was performed and the results are shown under each band. The OPTN amounts in each fraction were normalized to the actin amount and then plotted. Sup., supernatant fraction, Ppt., precipitated fraction.

The enhanced affinity of TBK1 to the E50K mutant protein affects the proper oligomerization and solubility of OPTN

To elucidate the factors that affect the solubility of OPTN, we first examined the native state of wild-type OPTN and the E50K mutant. FLAG-tagged OPTN was expressed in cells and lysates were routinely prepared without detergent and separated by native-polyacrylamide gel electrophoresis (PAGE). Western blotting analysis after native-PAGE indicated more E50K-protein complexes compared with those formed by wild-type OPTN (Fig. 5A) The complexes were immunoprecipitated (IP) using an anti-FLAG antibody and then separated by SDS–PAGE, which revealed distinct binding partners of OPTN and E50K (Fig. 5B, OPTN, white arrowheads; E50K, black arrowheads). We identified each binding partner by liquid chromatography–tandem mass spectrometry (LC–MS/MS). The OPTN partner was identified as OPTN itself, indicating tight oligomerization, while the E50K protein partner was identified as TBK1, which has been previously shown to interact with OPTN by a yeast two-hybrid screening (31). Each candidate interacting partner was further confirmed by IP and western blotting (Fig. 5C and D). Intriguingly, E50K exhibited enhanced affinity to TBK1, while its self-oligomerization was largely decreased (Fig. 5C, arrowhead). Oligomerized OPTN bands clearly seen in wild-type OPTN were restored by treatment with intracellular degradation inhibitors (Supplementary Material, Fig S7A, left panel, Oligomer lanes), indicating the importance of OPTN oligomerization in intracellular traffic and intracellular degradation. In contrast, these intracellular inhibitors had no effect on the diminished oligomerization of the E50K mutant (Supplementary Material, Fig. S7A right panel, Oligomer lanes). Treatment with a specific inhibitor treatment for TBK1, BX975 (32), was used to examine the relevance of TBK1 binding and the abnormal insolubility of the E50K mutant. BX795 treatment had no effects on the trace amounts of either wild-type OPTN (Supplementary Material, Fig. S7B) or calnexin in the Ppt. fraction (Fig. 5E); on the other hand, the amount of the insolubilized E50K mutant in the Ppt. fraction was drastically decreased by treatment with BX795 in a concentration-dependent manner. Prolonged BX795 treatment was able to restore the E50K mutant protein to the Sup. fraction (Fig 5F). These findings indicate that the enhanced affinity of E50K for TBK1 is one of the initial pathogenic events that trigger the intracellular insolubility of OPTN leading to improper OPTN transition from the ER to the Golgi body.

DISCUSSION

The OPTN E50K mutation is the only mutation currently affirmed as causative for NTG, and therefore, it is a clinically relevant mutation for elucidating the mechanism of disease onset at a molecular level (4). Although the E50K mutation is a rare event in familial POAG, the pathology is usually progressive, leading to full blindness even under strict IOP control (Supplementary Material, Fig. S1) (17). Previous reports on E50K mutant phenotypes were focused mainly on *in vitro* models using over-expression studies Though our initial report on the phenotypic analyses of E50K^{-tg} mice was informative (19), there is a strong necessity for further establishment of the model for OPTN and its target molecules in the endogenous

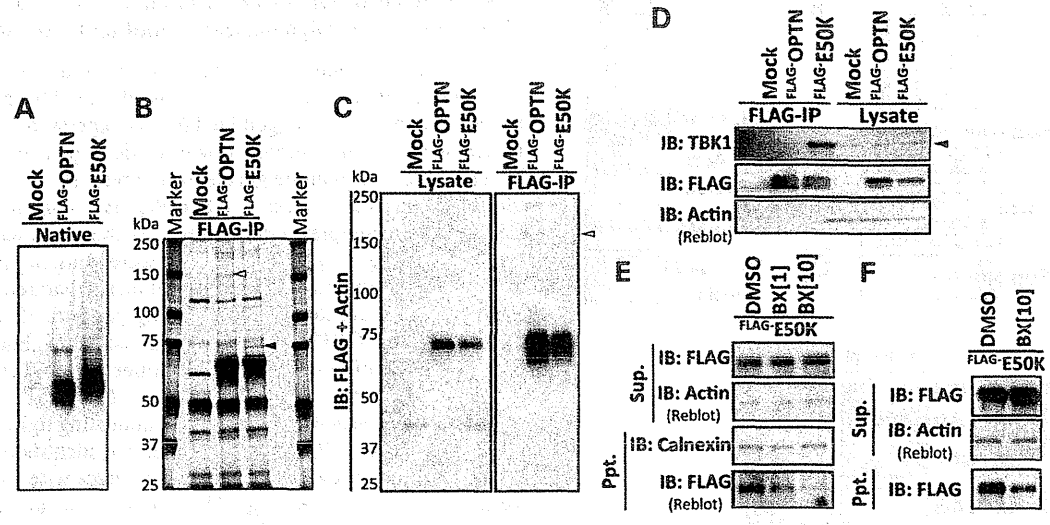

Figure 5. Constitutive interaction of the E50K mutant protein and TBK1 evokes the aberrant solubility of OPTN (**A**) Native-PAGE of mock-transfected controls, wild-type OPTN-transfected cells and E50K-transfected cells revealed the distinct protein complex formation. (**B**) Silver-staining of immunoprecipitates of mock-transfected controls, wild-type OPTN-transfected cells and E50K-transfected cells using an antibody specific for the FLAG-tag. The relevant bands, wild-type OPTN-specific binding molecule (white arrowhead) and E50K mutant-specific binding molecule (black arrowhead), were detected and further analyzed with LC–MS/MS. (**C**) Oligomerization of OPTN. The band indicated with white arrowhead in (B) turned out OPTN itself, i.e. wild-type OPTN is able to oligomerize, while E50K mutant protein largely lacks this oligomerization ability (**D**) E50K mutant and TBK1 interaction. The band indicated with black arrowhead in (B) turned out TBK1 and E50K mutant protein exhibited higher affinity to TBK1 protein than wild-type OPTN (**E**) The treatment with BX795, a TBK1 inhibitor, decreases the aberrant precipitation of E50K mutant protein in the Ppt. fraction in a concentration-dependent manner. Dimethylsulfoxide (DMSO) was used as the vehicle control and BX [1], BX [10] indicates the BX795 treatment concentrations of 1 μg/ml and 10 μg/ml, respectively, for 3 h. (**F**) Longer treatment with BX795 (6 h with 10 μg/ml) suppressed aberrant precipitation of E50K mutant protein in the Ppt. fraction and simultaneously restored E50K to the soluble fraction.

context to understand the exact molecular functions of OPTN and its mutations in glaucoma. In addition to the previously identified glaucomatous phenotypes, such as RGC loss, E50K^{-tg} mice also exhibit prominent retinal reactive gliosis with GFAP-positive Müller cells. It has been reported that GFAP-positive Müller cells can be experimentally induced in animal models mimicking glaucomatous phenotypes through various retinal insults, such as axonal damage, intravitreal injection and laser ablation (22–24). Thus, the persistent gliosis and inner layer cell death in E50K^{-tg} mice, without elevation of IOP, were of great interest, and this suggests that increased IOP is not the sole cause for POAG. The deposit-like E50K mutant protein seen in the INL of the retinas of E50K^{-tg} mice was encouraging, because similar abnormal protein inclusions are frequently found in clinical specimens of neurodegenerative tissues, including ALS (20, 33). Why E50K expression, which occurs throughout the body, only affects retinal homeostasis remains unknown. OPTN is also endogenously expressed in many other types of cells, like fibroblasts (7). In addition, most of the other cells expressing OPTN are proliferative and replaced usually within a few months, whereas the neural cells are usually non-proliferative and long-lived. We surmise that this is why the accumulation of E50K over time is critical in the pathogenesis of neurodegenerative diseases, including NTG. Though the E50K^{-tg} mice exhibit some representative neurodegenerative disease phenotypes, further investigation of the E50K accumulation in the endogenous context over time *in vivo* in the retina is needed, preferable in retinal specimens from E50K mutation-carrying NTG patient or from a mouse model, such as a site-specific knock-in mouse model.

Previous *in vitro* studies on E50K have shown large vesicle formation and Golgi fragmentation (10, 20), while there are no reports of endogenous E50K localization and behavior, especially in patient neuronal cells. In general, data pertaining to OPTN in clinical samples of patients with neurodegenerative diseases, including the retinal disease, is scarce. The iPSC technology is one solution to overcome this longstanding limitation by indirectly generating the desired target cells from iPSCs derived from patients with genetically driven neurodegenerative diseases (34). With this first report of the establishment of E50K-glaucoma iPSCs and their neuronal induction, molecular and cellular characterization of POAG onset can now be studied in the endogenous context. iPSC-derived neural cells from E50K mutation-carrying patients revealed for the first time that OPTN accumulated at the constricted Golgi body. In our current experiments, unlike the results of the E50K over-expression studies, Golgi was constricted but not fragmented. This discrepancy should be carefully examined to elucidate whether fragmentation of Golgi body is an endogenous phenotype or just an artifact induced by the over-expression. In any case, excess accumulation of E50K triggers Golgi body deformation and further deteriorates intracellular traffic, and eventually leads to cell death. It is well known that OPTN has a role in secretory vesicle transport and that E50K expression decreases the release of the neurotrophic factor NT3 (9, 35). Furthermore, prostaglandin E2 (PGE2) release via exocytosis is also decreased by E50K expression (Supplementary Material, Fig. S1B). These results indicate that due to the intracellular transport failure in cells expressing the E50K mutant, the paracrine activity for cellular protection and blood flow within the retina would also be attenuated.

Retinal vessel vulnerability in E50K^{-tg} mice is explained by these indirect extracellular E50K effects.

This study demonstrated that the E50K mutant is insoluble and is associated with the hydrophobic precipitate in lysates, compared with the wild-type OPTN, in iPSCs and iPSC-derived neural cells. Abnormal protein deposits, as shown in the retinas of the E50K^{-tg} mice, and protein hydrophobicity are frequently reported in neurodegenerative diseases (36–38). Recent reports in yeast models also supported the distinct hydrophobicities of wild-type OPTN and the E50K mutant (39). Although the prediction of isoelectric points (Compute pI/Mw, ExPASy) of wild-type OPTN and E50K do not differ (OPTN = 5.21, E50K = 5.26), their intracellular protein complex formation is considerably different. The amino acid characteristic of hydrophobic glutamate (E) against hydrophilic lysine (K) suggests that the E50K mutation is a possible charge swap mutation. E50K is located adjacent to the coiled-coil domain, which is a domain implicated in the interaction between OPTN and TBK1 (31, 15). The hydrophobicity of the E50K mutant was closely related with its enhanced interaction with TBK1, a well-known infection-responsive molecule. TBK1 induces macroautophagy by interacting with wild-type OPTN only under conditions of infection, and mediates crosstalk between innate immune response and autophagy (15). Additionally, the copy number variation of *TBK1* was associated with NTG onset (5, 6). The duplication of genes on chromosome 12q14 with familial POAG suggested that an extra copy of the *TBK1* gene and its copy number variation were responsible for NTG (40). More recently, NTG-related TBK1 mutations were also reported (41) Thus it is now well established that both *OPTN* and *TBK1* missense mutations are related with NTG onset. The abnormal physical protein interaction with TBK1 is responsible for the major cause of NTG in relation to the OPTN-E50K mutation. Together with the clinical facts, it has been reported that TBK1 has an important role in innate immunity pathways, and phosphorylated the ER-resident adaptor protein stimulator of IFN genes (STING) to enable IFN production (42, 43). Complexes of these molecules may be involved with the failure of the E50K OPTN protein to transition from ER to Golgi. Although TBK1 contributes to infection-related immunological responses, it also seems to contribute to the intracellular clearance of unnecessary components, such as by autophagy (15). Many other ophthalmic diseases, like macular diseases, are associated with abnormal protein metabolism (44); thus, the crosstalk of OPTN and TBK1 in the maintenance of intracellular clearance in retinal cells is likely to play a significant role in not only glaucomatous but also various other retinal diseases. Even though the exact function of TBK1 and the mechanism of the OPTN-TBK1 crosstalk in retinal homeostasis needs to be elucidated, compounds that abrogate the interaction between the E50K mutant and TBK1 are likely to be beneficial in the treatment of NTG patients.

Our current results pinpoint the molecular basis and concepts of NTG onset in E50K mutation-carrying patients and suggest that the RGC loss, the hallmark of glaucoma, is rather a terminal consequence of the sequential events, i.e. altered affinity of the E50K mutant inhibits self-oligomerization, leading to increased hydrophobicity, which affects downstream functions of OPTN, and eventually leads to cell death. Chronic and excessive accumulation of the E50K mutant protein recapitulated the partial neurodegenerative pathology, including reactive gliosis, vulnerability of retinal vessels and increased apoptotic cell death.

RGC loss is a hallmark of glaucoma; however, the results of this study showed that this phenomenon in E50K-NTG model is at the terminal stage of sequential abnormal events in the retina. In-depth characterization of the mutant protein in a physiologically relevant context and the proper choice/availability of a suitable animal model will help to elucidate and explore therapeutics for personalized treatment of glaucoma in the future.

MATERIALS AND METHODS

Antibodies and biochemical analysis

All the antibodies for biochemical studies were purchased from the following companies: anti-OPTN antibody (Cayman); anti-TBK1 antibody (Cell Signaling Technology); anti-FLAG (Sigma); anti-HA (Roche) and anti-Actin (Millipore). The TBK1 inhibitor, BX795, and cycloheximide were purchased from Calbiochem. Mini-PROTEAN TGX Gel and Transblot turbo system (BioRad) were used for native and SDS–PAGE western blotting according to the manufacturer's instructions. Quantitative western blotting was performed with ChemiDoc XRS+ with the Image lab software package (Biorad).

Animal experiments, preparation of retinal flat-mounts for staining and immunohistochemistry

All animal experiments were carried out in accordance with the Guide for the Care and Use of Laboratory Animals (National Institutes of Health) and the Association for Research in Vision and Ophthalmology Statement for the Use of Animals in Vision Research and approved by the Tokyo Medical Center Experimental Animal Committee. The OPTN mutant E50K^{-tg} mouse used in this study has been described previously (19). Twenty-two to 24-month-old male E50K^{-tg} mice ($n = 4$) and their littermates ($n = 4$) were sacrificed for the assessment of retinal gliosis. Both eyes were dissected and immunostained in flat-mounts as previously described (19). Briefly, dissected eyes were fixed in 2% paraformaldehyde and permeabilized with 0.1% Triton-phosphate-buffered saline (PBS). Non-specific binding was prevented by blocking with DAKO's serum-free blocking buffer, and all specimens were incubated with Alex488-conjugated anti-GFAP antibody (Millipore) for 4°C, over two nights. After radial dissection, retinas were mounted in DAKO's fluorescent mounting medium. A total of 16 retinal specimens, with four micrographs per one retinal specimen, were imaged by LSM700 confocal fluorescence microscopy (Zeiss) using a blinded method. Image analysis was conducted using the ZEN software (Zeiss) and the GFAP-positive area per retinal area was scored. The anti-OPTN (Cayman) and anti-HA (COVANCE) antibodies were used under heated antigen-retrieval conditions. Endogenous peroxidase was quenched by 3% H_2O_2 in MeOH. After primary antibody reaction for 4°C overnight, simple rabbit IgG-horse radish peroxidase (HRP) stain and mouse IgG-HRP stain for mouse tissue (Nichirei) were used as secondary HRP-conjugated polymers. After developing with 3,3′-diaminobenzidine (DAB) substrate, specimens were counter-stained with Gill's hematoxylin.

Light microscopy was performed with an Eclipse 600 microscope (Nikon).

Cell culture, transfection and immunocytochemistry

HEK293T cells were cultured in Dulbecco's modified Eagle medium (DMEM), supplemented with 10% heat-inactivated FBS The TransIT-PRO Transfection Kit (Mirus) was used according to the manufacturer's instructions. HEK293T cells were transfected with pAC-^{GFP}, pAC-^{GFP}-OPTN and pAC-^{GFP}-E50K to assess the intracellular localization of tagged OPTN. The ER-ID Red assay kit (Enzo) was used for endoplasmic reticulum staining. Anti-GM130 and Alexa633-conjugated anti-mouse IgG antibodies were used for Golgi immunostaining. The following constructs were used for over-expression studies: pEF-BOS-^{FLAG} (45), pEF-BOS-^{FLAG}-Optineurin and pEF-BOS-^{FLAG}-E50K.

Generation of iPSC and induction of differentiation to neural cells

Human E50K mutation-carrying iPSCs and the corresponding control iPSCs were established by Sendai-viral (DNAVEC) infection as previously reported (46) from circulating T-cells in the peripheral blood of human familial glaucoma patients with fully informed consent. All procedures were approved by the Ethics Committee of National Hospital Organization Tokyo Medical Center. For maintaining the pluripotency, iPSCs were cultured in bovine fibroblast growth factor (bFGF)-containing iPSC media on Matrigel-coated culture dishes. Oct3 and Nanog were used as pluripotency markers and Tuj1 was used as the neuronal marker Neural cell induction was performed via embryoid body formation as described previously (27, 28), utilizing the Neuron differentiation Kit (R&D Systems) in accordance with the manufacturer's procedures.

Identification of E50K-binding proteins by LC–MS/MS

Samples for LC–MS/MS analysis were prepared by preparing lysates from HEK293T cells over-expressing FLAG-tagged OPTN from pEF-BOS-^{FLAG}, pEF-BOS-^{FLAG}-Optineurin or pEF-BOS-^{FLAG}-E50K. Each lysate sample was immunoprecipitated with M2-FLAG-Agarose (Sigma) for 2 h at 4°C. The immunoprecipitated beads were washed with lysis buffer five times and then eluted with 2 M urea. The eluates were electrophoresed on 7.5% SDS–PAGE gels and the gels were silver-stained with the Silver Quest Kit (Invitrogen). The band of interest was processed for in-gel digestion for further LC–MS/MS analysis. Samples were analyzed with LCQ-DECA XP (Thermo Scientific). The obtained binding candidates and their interaction with OPTN/E50K were confirmed by immunoprecipitation and western blotting.

SUPPLEMENTARY MATERIAL

Supplementary Material is available at HMG online.

FUNDING

This work was supported by grants to T.I. by the Japanese Ministry of Health, Labour and Welfare (10103254), National Hospital Organization of Japan and the Japan Society for the Promotion of Science (09005752 to T.I., 24791885 to Y.M.). The pEF-BOS vector was a kind gift from Dr Seisuke Hattori in Kitasato University.

AUTHOR CONTRIBUTIONS

Y.M. and T.I designed the study; Y.M., D.I., H.K., Z.-L C., H.K., performed the experiments; K.K., T.Y., T.S., S.Y , K.F. contributed new reagents/techniques; Y.M. and T.I. analyzed the data; Y.M. and T.I. wrote the paper.

REFERENCES

1 Quigley, H.A. and Broman, A.T (2006) The number of people with glaucoma worldwide in 2010 and 2020. *Br J Ophthalmol.*, **90**, 262–267
2 Quigley, H.A. (2011) Glaucoma. *Lancet*, **377**, 1367–1377.
3. Suzuki, Y , Iwase, A., Araie, M., Yamamoto, T., Abe, H., Shirato, S., Kuwayama, Y., Mishima, H.K., Shimizu, H., Tomita, G *et al.* (2006) Risk factors for open-angle glaucoma in a Japanese population. the Tajimi Study. *Ophthalmology*, **113**, 1613–1617
4. Iwase, A., Suzuki, Y., Araie, M., Yamamoto, T., Abe, H., Shirato, S., Kuwayama, Y., Mishima, H.K., Shimizu, H., Tomita, G. *et al.* (2004) The prevalence of primary open-angle glaucoma in Japanese: the Tajimi Study *Ophthalmology*, **111**, 1641–1648.
5 Fingert, J.H., Robin, A.L., Stone, J.L., Roos, B.R., Davis, L.K., Scheetz, T.E , Bennett, S.R., Wassink, T H., Kwon, Y.H., Alward, W.L. *et al.* (2011) Copy number variations on chromosome 12q14 in patients with normal tension glaucoma. *Hum. Mol. Genet.*, **20**, 2482–2494.
6. Kawase, K., Allingham, R.R., Meguro, A., Mizuki, N., Roos, B., Solivan-Timpe, F.M., Robin, A.L., Ritch, R. and Fingert, J.H. (2012) Confirmation of TBK1 duplication in normal tension glaucoma. *Exp. Eye Res.*, **96**, 178–180.
7. Rezaie, T., Child, A., Hitchings, R., Brice, G., Miller, L., Coca-Prados, M., Heon, E., Krupin, T., Ritch, R., Kreutzer, D *et al.* (2002) Adult-onset primary open-angle glaucoma caused by mutations in optineurin. *Science*, **295**, 1077–1079
8 Sahlender, D.A., Roberts, R.C., Arden, S.D., Spudich, G., Taylor, M.J., Luzio, J.P., Kendrick-Jones, J. and Buss, F (2005) Optineurin links myosin VI to the Golgi complex and is involved in Golgi organization and exocytosis. *J Cell Biol.*, **169**, 285–295.
9 Bond, L.M., Peden, A.A., Kendrick-Jones, J , Sellers, J.R. and Buss, F (2011) Myosin VI and its binding partner optineurin are involved in secretory vesicle fusion at the plasma membrane. *Mol. Biol. Cell*, **22**, 54–65.
10. Park, B.C., Shen, X., Samaraweera, M. and Yue, B.Y (2006) Studies of optineurin, a glaucoma gene: Golgi fragmentation and cell death from overexpression of wild-type and mutant optineurin in two ocular cell types. *Am. J Pathol.*, **169**, 1976–1989.
11 Nagabhushana, A., Chalasani, M.L., Jain, N , Radha, V., Rangaraj, N., Balasubramanian, D. and Swarup, G. (2010) Regulation of endocytic trafficking of transferrin receptor by optineurin and its impairment by a glaucoma-associated mutant. *BMC Cell Biol.*, **11**, 4.
12. Chalasani, M.L., Radha, V., Gupta, V., Agarwal, N., Balasubramanian, D. and Swarup, G (2007) A glaucoma-associated mutant of optineurin selectively induces death of retinal ganglion cells which is inhibited by antioxidants. *Invest. Ophthalmol. Vis. Sci.*, **48**, 1607–1614.
13 Meng, Q., Lv, J., Ge, H., Zhang, L., Xue, F., Zhu, Y. and Liu, P. (2012) Overexpressed mutant optineurin(E50K) induces retinal ganglion cells apoptosis via the mitochondrial pathway. *Mol. Biol. Rep.*, **39**, 5867–5873
14. Gleason, C.E., Ordureau, A., Gourlay, R., Arthur, J.S. and Cohen, P (2011) Polyubiquitin binding to optineurin is required for optimal activation of TANK-binding kinase 1 and production of interferon beta. *J. Biol. Chem.*, **286**, 35663–35674.
15 Wild, P., Farhan, H., McEwan, D G., Wagner, S., Rogov, V V., Brady, N.R., Richter, B., Korac, J., Waidmann, O., Choudhary, C. *et al.* (2011)

Phosphorylation of the autophagy receptor optineurin restricts Salmonella growth. *Science*, **333**, 228–233.
16. Ying, H. and Yue, B.Y. (2012) Cellular and molecular biology of optineurin. *Int. Rev. Cell. Mol. Biol.*, **294**, 223–258.
17. Aung, T., Rezaie, T , Okada, K., Viswanathan, A.C., Child, A.H., Brice, G., Bhattacharya, S.S., Lehmann, O.J., Sarfarazi, M. and Hitchings, R.A. (2005) Clinical features and course of patients with glaucoma with the E50K mutation in the optineurin gene. *Invest. Ophthalmol. Vis. Sci.*, **46**, 2816–2822.
18. Hauser, M.A., Sena, D.F., Flor, J., Walter, J., Auguste, J., Larocque-Abramson, K., Graham, F., Delbono, E., Haines, J.L., Pericak-Vance, M.A. *et al.* (2006) Distribution of optineurin sequence variations in an ethnically diverse population of low-tension glaucoma patients from the United States. *J. Glaucoma*, **15**, 358–363
19. Chi, Z.L., Akahori, M., Obazawa, M., Minami, M., Noda, T., Nakaya, N., Tomarev, S., Kawase, K., Yamamoto, T., Noda, S. *et al.* (2010) Overexpression of optineurin E50K disrupts Rab8 interaction and leads to a progressive retinal degeneration in mice. *Hum. Mol. Genet.*, **19**, 2606–2615
20. Maruyama, H., Morino, H., Ito, H., Izumi, Y , Kato, H., Watanabe, Y., Kinoshita, Y., Kamada, M., Nodera, H., Suzuki, H. *et al.* (2010) Mutations of optineurin in amyotrophic lateral sclerosis. *Nature*, **465**, 223–226.
21 Ganesh, B.S. and Chintala, S.K. (2011) Inhibition of reactive gliosis attenuates excitotoxicity-mediated death of retinal ganglion cells. *PLoS One*, **6**, e18305
22. Wurm, A., Iandiev, I., Uhlmann, S., Wiedemann, P., Reichenbach, A., Bringmann, A. and Pannicke, T (2011) Effects of ischemia-reperfusion on physiological properties of Muller glial cells in the porcine retina. *Invest. Ophthalmol. Vis. Sci.*, **52**, 3360–3367.
23 Giani, A., Thanos, A., Roh, M.I., Connolly, E., Trichonas, G., Kim, I., Gragoudas, E., Vavvas, D. and Miller, J.W (2011) In vivo evaluation of laser-induced choroidal neovascularization using spectral-domain optical coherence tomography *Invest. Ophthalmol. Vis. Sci.*, **52**, 3880–3887
24. Ueda, K., Nakahara, T , Hoshino, M., Mori, A., Sakamoto, K. and Ishii, K. (2010) Retinal blood vessels are damaged in a rat model of NMDA-induced retinal degeneration. *Neurosci. Lett.*, **485**, 55–59.
25. Lasiecka, Z.M. and Winckler, B. (2011) Mechanisms of polarized membrane trafficking in neurons – focusing in on endosomes. *Mol. Cell. Neurosci.*, **48**, 278–287
26. Farhan, H., Freissmuth, M. and Sitte, H.H. (2006) Oligomerization of neurotransmitter transporters: a ticket from the endoplasmic reticulum to the plasma membrane. *Handb. Exp. Pharmacol.*, **175**, 233–249
27 Tsuji, O., Miura, K., Okada, Y., Fujiyoshi, K., Mukaino, M., Nagoshi, N., Kitamura, K., Kumagai, G., Nishino, M., Tomisato, S. *et al.* (2010) Therapeutic potential of appropriately evaluated safe-induced pluripotent stem cells for spinal cord injury. *Proc. Natl Acad. Sci. USA*, **107**, 12704–12709.
28. Tucker, B.A., Scheetz, T.E., Mullins, R.F., DeLuca, A.P., Hoffmann, J.M , Johnston, R.M., Jacobson, S.G., Sheffield, V.C. and Stone, E.M. (2011) Exome sequencing and analysis of induced pluripotent stem cells identify the cilia-related gene male germ cell-associated kinase (MAK) as a cause of retinitis pigmentosa. *Proc. Natl Acad. Sci. USA*, **108**, E569–576.
29. Sarfarazi, M. and Rezaie, T (2003) Optineurin in primary open angle glaucoma. *Ophthalmol. Clin. North Am.*, **16**, 529–541
30. Shen, X., Ying, H., Qiu, Y., Park, J.S., Shyam, R., Chi, Z.L., Iwata, T and Yue, B.Y (2011) Processing of optineurin in neuronal cells. *J. Biol. Chem.*, **286**, 3618–3629.
31. Morton, S., Hesson, L., Peggie, M. and Cohen, P (2008) Enhanced binding of TBK1 by an optineurin mutant that causes a familial form of primary open angle glaucoma. *FEBS Lett.*, **582**, 997–1002.
32. Clark, K., Plater, L., Peggie, M. and Cohen, P. (2009) Use of the pharmacological inhibitor BX795 to study the regulation and physiological roles of TBK1 and IkappaB kinase epsilon: a distinct upstream kinase mediates Ser-172 phosphorylation and activation. *J. Biol. Chem.*, **284**, 14136–14146.
33 Ito, H., Nakamura, M., Komure, O., Ayaki, T., Wate, R., Maruyama, H., Nakamura, Y., Fujita, K., Kaneko, S., Okamoto, Y. *et al.* (2011) Clinicopathologic study on an ALS family with a heterozygous E478G optineurin mutation. *Acta Neuropathol.*, **122**, 223–229
34. Imaizumi, Y., Okada, Y., Akamatsu, W., Koike, M., Kuzumaki, N., Hayakawa, H., Nihira, T , Kobayashi, T., Ohyama, M., Sato, S. *et al.* (2012) Mitochondrial dysfunction associated with increased oxidative stress and alpha-synuclein accumulation in PARK2 iPSC-derived neurons and postmortem brain tissue. *Mol. Brain*, **5**, 35
35 Sippl, C., Bosserhoff, A.K., Fischer, D. and Tamm, E.R. (2011) Depletion of optineurin in RGC-5 cells derived from retinal neurons causes apoptosis and reduces the secretion of neurotrophins. *Exp. Eye Res.*, **93**, 669–680.
36. Nukina, N., Kosik, K.S. and Selkoe, D.J (1987) Recognition of Alzheimer paired helical filaments by monoclonal neurofilament antibodies is due to crossreaction with tau protein. *Proc. Natl Acad. Sci. USA*, **84**, 3415–3419
37 Hoffner, G., Kahlem, P and Djian, P (2002) Perinuclear localization of huntingtin as a consequence of its binding to microtubules through an interaction with beta-tubulin. relevance to Huntington's disease. *J Cell Sci.*, **115**, 941–948.
38 LaVoie, M.J., Ostaszewski, B.L., Weihofen, A., Schlossmacher, M.G and Selkoe, D.J. (2005) Dopamine covalently modifies and functionally inactivates parkin. *Nat. Med.*, **11**, 1214–1221.
39 Kryndushkin, D., Ihrke, G , Piermartiri, T C. and Shewmaker, F (2012) A yeast model of optineurin proteinopathy reveals a unique aggregation pattern associated with cellular toxicity. *Mol. Microbiol.*, **86**, 1531–1547
40. Fingert, J.H., Darbro, B.W , Qian, Q., Van Rheeden, R., Miller, K., Riker, M., Solivan-Timpe, F., Roos, B.R., Robin, A.L. and Mullins, R.F. (2013) TBK1 and flanking genes in human retina. *Ophthalmic Genet.*, doi.10.3109/13816810.2013.768674.
41 Seo, S., Solivan-Timpe, F , Roos, B.R., Robin, A.L., Stone, E.M., Kwon, Y.H., Alward, W.L. and Fingert, J.H. (2013) Identification of proteins that interact with TANK binding kinase 1 and testing for mutations associated with glaucoma. *Curr Eye Res.*, **38**, 310–315
42. Saitoh, T., Fujita, N., Hayashi, T., Takahara, K., Satoh, T., Lee, H., Matsunaga, K., Kageyama, S., Omori, H., Noda, T *et al.* (2009) Atg9a controls dsDNA-driven dynamic translocation of STING and the innate immune response. *Proc. Natl Acad. Sci. USA*, **106**, 20842–20846.
43 Tanaka, Y. and Chen, Z.J. (2012) STING specifies IRF3 phosphorylation by TBK1 in the cytosolic DNA signaling pathway. *Sci. Signal.*, **5**, ra20.
44 Shaw, P.X., Zhang, L., Zhang, M., Du, H., Zhao, L., Lee, C., Grob, S., Lim, S.L., Hughes, G., Lee, J. *et al.* (2012) Complement factor H genotypes impact risk of age-related macular degeneration by interaction with oxidized phospholipids. *Proc. Natl Acad. Sci. USA*, **109**, 13757–13762
45 Mizushima, S. and Nagata, S (1990) pEF-BOS, a powerful mammalian expression vector. *Nucleic Acids Res.*, **18**, 5322.
46. Seki, T., Yuasa, S., Oda, M., Egashira, T., Yae, K., Kusumoto, D., Nakata, H., Tohyama, S., Hashimoto, H., Kodaira, M. *et al.* (2010) Generation of induced pluripotent stem cells from human terminally differentiated circulating T cells. *Cell Stem Cell*, **7**, 11–14.

CLINICAL CHARACTERISTICS OF OCCULT MACULAR DYSTROPHY IN FAMILY WITH MUTATION OF *RP1L1* GENE

KAZUSHIGE TSUNODA, MD, PHD,* TOMOAKI USUI, MD, PHD,†‡ TETSUHISA HATASE, MD, PHD,† SATOSHI YAMAI, MD,§ KAORU FUJINAMI, MD,* GEN HANAZONO, MD, PHD,* KEI SHINODA, MD, PHD,*¶ HISAO OHDE, MD, PHD,** MASAKAZU AKAHORI, PHD,* TAKESHI IWATA, PHD,* YOZO MIYAKE, MD, PHD*††

Purpose: To report the clinical characteristics of occult macular dystrophy (OMD) in members of one family with a mutation of the *RP1L1* gene.

Methods: Fourteen members with a p.Arg45Trp mutation in the *RP1L1* gene were examined. The visual acuity, visual fields, fundus photographs, fluorescein angiograms, full-field electroretinograms, multifocal electroretinograms, and optical coherence tomographic images were examined. The clinical symptoms and signs and course of the disease were documented.

Results: All the members with the *RP1L1* mutation except one woman had ocular symptoms and signs of OMD. The fundus was normal in all the patients during the entire follow-up period except in one patient with diabetic retinopathy. Optical coherence tomography detected the early morphologic abnormalities both in the photoreceptor inner/outer segment line and cone outer segment tip line. However, the multifocal electroretinograms were more reliable in detecting minimal macular dysfunction at an early stage of OMD.

Conclusion: The abnormalities in the multifocal electroretinograms and optical coherence tomography observed in the OMD patients of different durations strongly support the contribution of *RP1L1* mutation to the presence of this disease

RETINA 32:1135–1147, 2012

Occult macular dystrophy (OMD) was first described by Miyake et al[1] to be a hereditary macular dystrophy without visible fundus abnormalities. Patients with OMD are characterized by a progressive decrease of visual acuity with normal-appearing fundus and normal fluorescein angiograms (FA). The important signs of OMD are normal full-field electroretinograms (ERGs) but abnormal focal macular ERGs and multifocal electroretinograms (mfERGs) also exist. These findings indicated that the retinal dysfunction was confined to the macula.[1–5] Optical coherence tomography (OCT) showed structural changes in the outer nuclear and photoreceptor layers.[6–11]

Recently, we found that dominant mutations in the *RP1L1* gene were responsible for OMD.[12] The *RP1L1* gene was originally cloned as a gene derived from common ancestors as a retinitis pigmentosa 1 (*RP1*) gene, which is responsible for 5–10% of autosomal dominant retinitis pigmentosa worldwide, on the same Chromosome 8.[13–17] A number of attempts have been made to identify mutations in *RP1L1* in various retinitis pigmentosa patients with no success. An immunohistochemical study on cynomolgus monkeys showed that *RP1L1* was expressed in rod and cone photoreceptors, and *RP1L1* is thought to play important roles in the morphogenesis of the photoreceptors.[13,18] Heterozygous *RP1L1* knockout mice were reported to be normal, whereas homozygous knockout mice develop subtle retinal degeneration.[18] However, the RP1L1 protein has a very low degree of overall sequence

From the *Laboratory of Visual Physiology, National Institute of Sensory Organs, Tokyo, Japan; †Division of Ophthalmology and Visual Science, Graduate School of Medical and Dental Sciences, Niigata University, Niigata, Japan; ‡Akiba Eye Clinic, Niigata, Japan, §Department of Ophthalmology, Sado General Hospital, Niigata, Japan; ¶Department of Ophthalmology, School of Medicine, Teikyo University, Tokyo, Japan; **Department of Ophthalmology, School of Medicine, Keio University, Tokyo, Japan; and ††Aichi Medical University, Aichi, Japan.

The authors have no financial interest or conflicts of interest.

Supported in part by research grants from the Ministry of Health, Labor and Welfare, Japan and Japan Society for the Promotion of Science, Japan.

Reprint requests: Kazushige Tsunoda, Laboratory of Visual Physiology, National Institute of Sensory Organs, 2-5-1 Higashigaoka, Meguro-ku, Tokyo 152-8902, Japan; e-mail. tsunodakazushige@kankakuki.go.jp

identity (39%) between humans and mice compared with the average values of sequence similarity observed between humans and mice proteins. The results of linkage studies have strongly supported the contribution of *RP1L1* mutations to the presence of this disease,[12] but the function of *RP1L1* in the human retina has not been completely determined.

A large number of cases of OMD have been reported[7,10,19]; however, we did not always find the same mutations in sporadic cases or in small families, which had less than three affected members. This led us to hypothesize that several independent mutations can lead to the phenotype of OMD, that is, OMD is not a single disease caused by a specific gene mutation, but may represent different diseases with similar retinal dysfunctions.

Thus, the aim of this study was to determine the characteristics of OMD by investigating the phenotypes of patients with the *RP1L1* mutation from a single Japanese family.

Patients and Methods

We investigated 19 members from a single Japanese family. A homozygous mutation, p.Arg45Trp in the *RP1L1* gene, was confirmed in 14 members,[12] and 13 of the 14 were diagnosed with OMD. Among the 14 members with a mutation in the *RP1L1* gene, 11 were followed-up at the Niigata University in Niigata, Japan. The other three were examined at the National Institute of Sensory Organs in Tokyo, Japan. Each member had a complete ophthalmic examination including best-corrected visual acuity (BCVA), refraction, perimetry, fundus photography, FA, full-field ERGs,[20] mfERGs,[21] and OCT. The visual fields were determined by Goldmann perimetry or by Humphrey Visual Field Analyzer (Model 750i; Carl Zeiss Meditec, Inc, Dublin, CA). The SITA Standard strategy was used with the 30-2 program or the 10-2 program for the Humphrey Visual Field Analyzer.

Electroretinograms were used to assess the retinal function under both scotopic and photopic conditions.[22] Full-field ERGs were recorded using the International Society of Clinical Electrophysiology and Vision standard protocol. Multifactorial electroretinograms were recorded with the Visual Evoked Response Imaging System (VERIS science 4.1; EDI, San Mateo, CA). A Burian–Allen bipolar contact lens electrode was used to record the mfERGs. The visual stimuli consisted of 61 or 103 hexagonal elements with an overall subtense of approximately 60°. The luminance of each hexagon was independently modulated between black (3.5 cd/m^2) and white (138.0 cd/m^2) according to a binary m-sequence at 75 Hz. The surround luminance was 70.8 cd/m^2.

The OCT images were obtained with a spectral-domain OCT (HD-OCT; Carl Zeiss Meditec or a 3D-OCT-1000, Mark II; Topcon) from 21 eyes of 12 cases in the same pedigree.

The procedures used adhered to the tenets of the Declaration of Helsinki and were approved by the Medical Ethics Committee of both the Niigata University and National Institute of Sensory Organs. An informed consent was received from all the subjects for the tests.

Results

The findings of 5 generations of 1 family with OMD are shown in Figure 1. The numbered family members had the same mutation in *RP1L1* (p.Arg45Trp), and family members designated with the filled squares or filled circles were phenotypically diagnosed with OMD by routine examinations including visual field tests, FA, mfERGs, and Fourier-domain OCT. Only Patient 5 (age 60 years) had normal phenotype, although she had the *RP1L1* mutation.

The clinical characteristics and the results of ocular examinations of all the 14 family members with the *RP1L1* mutation (p.Arg45Trp) are listed in Tables 1 and 2. Family Member #5 was diagnosed as normal because she had normal mfERGs.

Among the 13 OMD patients (average age at the final examination, 57.2 ± 22.1 years), 12 complained of disturbances of central vision and 4 complained of photophobia (Table 1). Patient 1 did not report any visual disturbances in the right eye as did Patient 6 for both eyes. The visual dysfunction in these eyes was confirmed by mfERGs. For 13 patients, the age at the onset of visual difficulties varied from 6 years to 50 years with a mean of 27.3 ± 15.1 years.

All the patients were affected in both eyes, and the onset was the same in the 2 eyes except for Patients 1, 11, 12, and 14. Patient 1 first noticed a decrease in her visual acuity in her left eye at age 50 years, and she still did not have any subjective visual disturbances in her right eye 30 years later. However, a clear decrease in the mfERGs in the macular area was detected in both eyes. Patient 11 first noticed a decrease in the visual acuity in her right eye at age 47 years when the BCVA was 0.2 in the right eye and 1.2 in the left eye (Figure 2). Seven years later at age 54 years, she noticed a decrease in the vision in her left eye. Similarly, Patients 12 and 14 did not report any visual disturbances in their right eyes until 2 (Patient 12) or 8 (Patient 14) years after the onset in their left eyes.

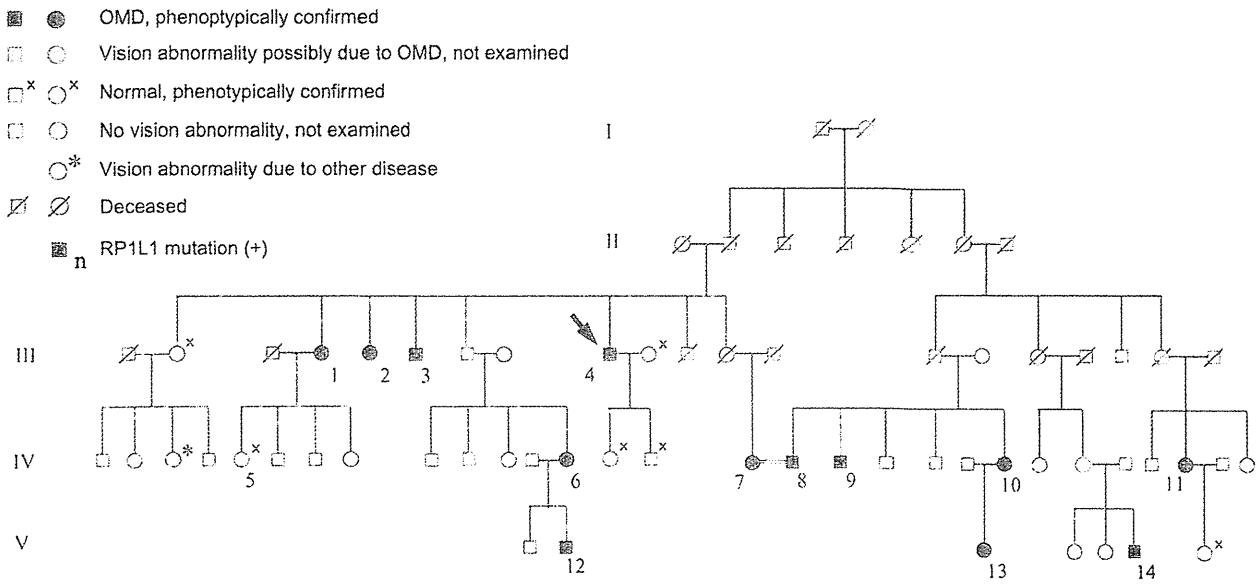

Fig. 1. Pedigree of a family with OMD. The identification number of the patients is marked beside the symbols. The proband is indicated by an arrow The open squares and circles with crosses are the relatives whose visual function was confirmed to be normal by routine examinations including Humphrey visual field tests, mfERGs, and Fourier-domain OCT Those designated by hatched squares or circles were reported to have poor vision with similar severity and onset as the other genetically confirmed OMD patients. One relative marked by an asterisk had unilateral optic atrophy because of retrobulbar neuritis

The duration of the continuous decrease in the BCVA varied from 10 years to 30 years (mean, 15.6 ± 7.7 years) in 16 eyes of 9 adult patients. After this period, these patients reported that their vision did not decrease. Patients 2, 3, 8, and 14 complained of photophobia, and the degree of photophobia remained unchanged after the visual acuity stopped decreasing. Patients 1, 2, 4, 7, and 9 had additional disturbances of vision because of senile cataracts, and Patients 2 and 4 had bilateral cataract surgery. The visual disturbances because of the OMD were still progressing at the last examination in the left eye of Patient 11 (age 57 years), and both eyes of Patient 12 (age 20 years), Patient 13 (age 18 years), and Patient 14 (age 28 years).

Different systemic disorders were found in some of the patients; however, there did not seem to be a specific disorder, which was common to all of them (Table 1).

In the 16 eyes of 9 patients whose BCVA had stopped decreasing, the BCVA varied from 0.07 to 0.5 (Table 2). The BCVA of the left eye of Patient 6 was 0.07 because of an untreated senile cataract. If this eye is excluded, the final BCVAs of all the stationary eyes range from 0.1 to 0.5. Patient 2 had photophobia, and her BCVA measured by manually presenting Landolt rings on separate cards under room light was 0.4 in the right eye and 0.5 in the left eye, which was better than that measured by a Landolt chart of 0.3 in the right eye and 0.3 in the left eye with background illumination.

For the 13 patients whose original refractions were confirmed, 11 of 26 eyes were essentially emmetropic (<± 0.5 diopters). Both eyes of Patients 1, 3, 4, 6, and 8 and the left eye of Patient 5 were hyperopic (+0.675 to +4.625 diopters). The right eye of Patient 7, the left eye of Patient 12, and both eyes of Patient 13 were moderately myopic (−0.625 to −2.75 diopters). These results indicate that there is no specific refraction associated with OMD patients in this family.

The visual fields were determined by Goldmann perimetry or Humphrey Visual Field Analyzer. All the patients had a relative central scotoma in both eyes except for Patient 1 whose right eye was normal by Goldmann perimetry. In all cases, no other visual field abnormalities were detected during the entire course of the disease. In the patients examined shortly after the onset, a relative central scotoma was not detected by Goldman perimetry and was confirmed by static perimetry.

The fundus of all except one eye was normal. The left eye of Patient 9 had background diabetic retinopathy. At the first consultation at age 46 years, Patient 9 did not have diabetes, and the funduscopic examination and FA revealed no macular abnormalities. At the age 66 years, there were few microaneurysms in the left macula away from the fovea; however, OCT did not show any diabetic changes such as macular edema. The OMD was still the main cause of visual acuity reduction in this patient.

Six patients consented to FA, and no abnormality was detected in the entire posterior pole of the eye. It is noteworthy that both the fundus and FA of Patient 4 were normal at the age 73 years, which was >50 years

Table 1. Clinical Characteristics of the Family Members With RP1L1 Mutation (p.Arg45Trp)

Case	Age and Gender	Chief Complaint	Affected Eye	Age at Onset (Years)	Duration of Continuous Decrease in BCVA (Years)	Duration After the Onset (Years)	Systemic Disorders
1	81, F	Decreased visual acuity	Bilateral*	50	20	31	Hypertension
2	71, F	Decreased visual acuity and photophobia	Bilateral	25	25	46	Diabetes mellitus since 64 years of age
3	74, M	Decreased visual acuity and photophobia	Bilateral	30	10	44	Hyperlipidemia, angina pectoris
4	83, M	Decreased visual acuity	Bilateral	20	10	63	Hypertension, Multiple cerebral infarction at 73 years of age
5	60, F	None	—†	—	—	—	—
6	50, F	None	Bilateral*	Unknown	Unknown	Unknown	—
7	69, F	Decreased visual acuity	Bilateral	50	10	19	—
8	69, M	Decreased visual acuity and photophobia	Bilateral	28	10	41	Hypertension since 67 years of age, Surgery for ossification of the posterior longitudinal ligament at 45 years of age
9	66, M	Decreased visual acuity	Bilateral	30	15	36	Diabetes mellitus since 63 years of age
10	58, F	Decreased visual acuity	Bilateral	10	30	48	Rheumatoid arthritis since 46 years of age, Bronchiectasis since 43 years of age
11	57, F	Decreased visual acuity	Bilateral ‡	47	OD, 10, OS, still progressing	10	—
12	20, M	Decreased visual acuity	Bilateral§	14	Still progressing	6	Atopic dermatitis
13	18, F	Decreased visual acuity	Bilateral	6	Still progressing	12	—
14	28, M	Decreased visual acuity and photophobia	Bilateral¶	18	Still progressing	10	—

*Patient 1 has subjective visual disturbance only in the left eye, and Patient 6 does not have any subjective visual disturbances in both eyes. The visual dysfunction was confirmed by mfERG.

†This woman has a mutation in RP1L1, but her visual function was confirmed normal after routine examinations including mfERG.

‡This patient noticed visual disturbance only in the right eye at 47 years of age. The visual disturbance in the left eye was first noticed at 54 years of age.

§This patient noticed visual disturbance only in the left eye at 14 years of age. The visual disturbance in the right eye was first noticed at 16 years of age.

¶This patient noticed visual disturbance only in the left eye at 18 years of age. The visual disturbance in OD was first noticed at 26 years of age.

Table 2. Results of Ocular Examinations of the Family Members With RP1L1 Mutation

Case	Age and Gender	BCVA at Final Visit		Refraction (D)*		Visual Field	Fundus Appearance	FA	Full-Field ERG	Relative Amplitude in mfERG at Fovea (Ring 1/Ring 5 or Ring 6)†	Other Ocular Disorders
		OD	OS	OD	OS						
1	81, F	1.2	0.1	+4.25	+4.625	Relative central scotoma, OS	Normal, OU	Normal, OU	NE	2.34, OD, 0.60, OS	Senile cataract, OU
2	71, F	0.4	0.5	Unknown‡	Unknown‡	Relative central scotoma, OU	Normal, OU	NE	NE	Not measurable, OU	Cataract surgery, OS at 58 years of age, OD at 69 years of age, Ptosis, OU
3	74, M	0.2	0.3	+2.875	+3.375	Relative central scotoma, OU	Normal, OU	NE	NE	Not measurable, OU	Laser peripheral iridotomy, OU at 73 years of age
4	83, M	0.2	0.2	+1.0	+1.625	Relative central scotoma, OU	Normal, OU	Normal, OU	Normal ISCEV standard protocol ERG, OU	Not measurable, OU	Cataract surgery, OU at 80 years of age
5	60, F	1.2	1.2	−0.25	+0.875	Normal, OU	Normal, OU	NE	NE	4.24, OD, NE, OS	—
6	50, F	1.2	1.2	+1.0	+1.0	Relative central scotoma, OU	Normal, OU	NE	NE	2.74, OD, 2.23, OS	—
7	69, F	0.1§	0.07§	−0.625	+0.25	Relative central scotoma, OU	Normal, OU	NE	Normal ISCEV standard protocol ERG, OU	Not measurable, OU	Senile cataract, OU
8	69, M	0.1	0.1	+1.125	+0.675	Relative central scotoma, OU	Normal, OU	NE	Normal ISCEV standard protocol ERG, OU	1.01, OD, 1.30, OS	—